Fermi National Accelerator Laboratory

FERMILAB-Conf-95/003-E

CDF

The CDF Upgrade

C. Newman-Holmes
For The CDF Collaboration

Fermi National Accelerator Laboratory
P.O. Box 500, Batavia, Illinois 60510

January 1995

Published Proceedings of the *4th International Conference on Advanced Technology and Particle Physics*, Como, Italy, October 3-7, 1994.

Disclaimer

CDF/PUB/CDF/PUBLIC/2930
FERMILAB-CONF-95/003-E

The CDF Upgrade

C. Newman-Holmes

Collider Detector at Fermilab
Fermi National Accelerator Laboratory
Batavia, IL 60510 USA

The Collider Detector at Fermilab will be upgraded to allow the detector to function at the higher luminosity anticipated with improvements to the Fermilab accelerator complex. The upgrades are described.

1. INTRODUCTION

The Collider Detector at Fermilab (CDF) has been used to study proton-antiproton collisions at the Fermilab Tevatron since 1985. Over the years, the detector has evolved steadily to increase its physics capability and to keep pace with improvements to the Tevatron [1]. Fermilab is currently building a new Main Injector accelerator which will lead to even larger luminosity values [2]. This paper describes upgrades to CDF that will allow us to exploit the higher luminosity of the Main Injector.

Table 1 shows how the $\bar{p}p$ luminosity at the Tevatron collider has evolved over the last seven years. We hope to collect about 1 fb^{-1} of data in the run beginning in 1998. There is a rich variety of physics topics that can be investigated with a data set of this size [3]. We mention only a sampling here. First is further study of the top quark. CDF has published the first evidence for the top quark [4]. With 1 fb^{-1} of data, we hope to measure the top quark mass to about 5 GeV/c^2. Improved measurement of the W mass is also an important physics goal. In the Standard Model, the W-Z mass difference is related to the top quark mass through radiative corrections. The W-Z mass difference also depends weakly on the Higgs mass. Since the Z mass is known very precisely from LEP, one can calculate a relationship between the W mass and the top quark mass. This is shown in Figure 1 along with both the current measurements of M_{top} and M_W and the uncertainties expected with 1 fb^{-1}. The uncertainty on the W mass is expected to go down to about 50 MeV/c^2. We see from Figure 1 that with uncertainties of this size on M_{top} and M_W, there is a powerful check of the consistency of the Standard Model.

Hadron collider experiments have produced a wealth of results in QCD. Future studies will include improved measurement of the parton distribution functions at small x, gluon distribution functions and photon production. We will also continue to search for physics beyond the Standard Model, including supersymmetry, leptoquarks and excited quarks.

CDF has shown that hadron collider experiments can do b physics [5]. We expect to continue to improve measurements of b cross sections and lifetimes. Several exclusive final states will be studied including decays of the Λ_b and the B_c. A study of $B\bar{B}$ mixing should be possible. More speculative are observation of CP violation in the b system and study of hadronic decays of b particles.

Table 1
Tevatron/CDF Progress

Run/Date	Typical L ($cm^{-2}sec^{-1}$)	$\int$Ldt (pb^{-1})	# $W \rightarrow e\,\nu$ detected
1987	$3x10^{29}$	0.025	22
1988-89	$1.6x10^{30}$	4	2600
Run Ia (1992-93)	$5x10^{30}$	20	14,000
Run Ib (1994-)	$1.2x10^{31}$	100	70,000
Run II (begins 1998)	$8x10^{31}$	1000	700,000

Published Proceedings 4th International Conference on Advanced Technology and Particle Physics, Como, Italy, October 3-7, 1994.

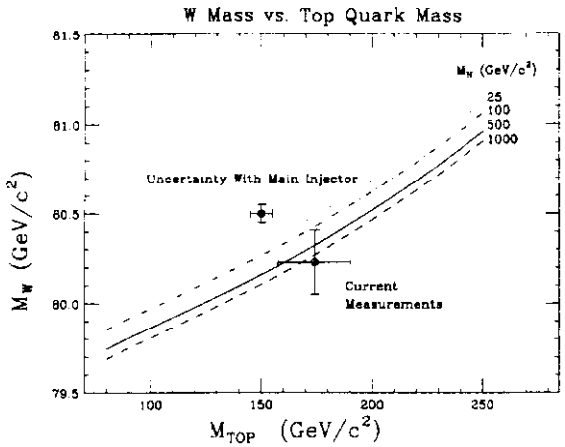

Figure 1. W mass vs. top quark mass for different values of the Higgs mass. Current measurements are shown as well as the uncertainties expected with 1 fb^{-1} of data.

2. THE CDF DETECTOR

A cross section of the CDF detector is shown in Figure 2 [6]. The detector currently (top of Figure 2) consists of a 1.4 Tesla superconducting solenoid with tracking detectors inside it. Calorimeters (electromagnetic and hadronic) are located outside the magnet and in the forward region. Muon detection is provided by chambers located outside the calorimeters in the central region, and by magnetized iron toroid spectrometers in the forward direction. A silicon vertex detector located just outside the beam pipe is used for secondary vertex identification [7]. With the planned upgrades to Fermilab accelerators, including the Main Injector, the luminosity is expected to reach ~ 10^{32} cm^{-2} sec^{-1}. The time between bunches will be reduced to 132 ns. CDF was designed for luminosity up to ~10^{30} cm^{-2} sec^{-1} and time between crossings = 3.5 μsec so many parts of the existing detector must be upgraded to work with the Main Injector. The current upgrade plans are to:

- Replace the plug and forward gas calorimeters with a new scintillator-based calorimeter;
- Replace the silicon vertex detector with a device with faster readout and larger acceptance;
- Upgrade the front-end electronics and trigger systems to accommodate data-taking at higher rates;
- Upgrade the data acquisition system to increase throughput and reliability.

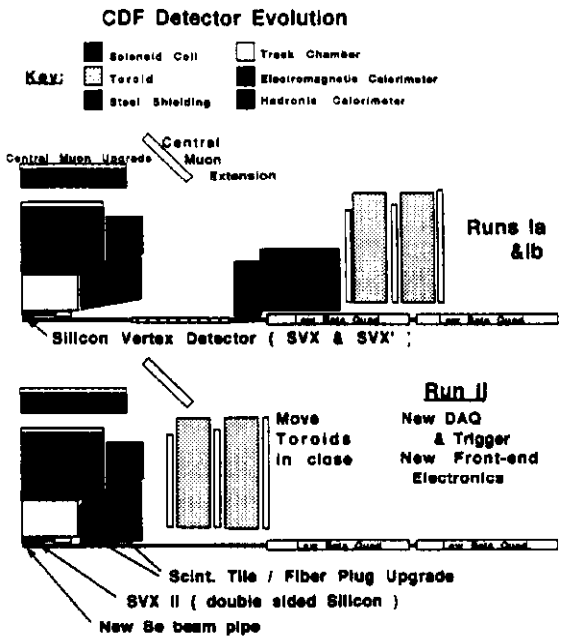

Figure 2. Evolution of CDF. The top figure shows the current configuration and the bottom figure shows the upgraded detector.

These projects are discussed in more detail below. Improvements to the muon systems are also planned, but these are straightforward extensions of the existing systems and will not be discussed here. In addition, the off-line computing capability must be enhanced to provide for efficient production of physics results as the quantity of data increases.

3. PLUG CALORIMETER

New calorimeters are being built to replace the gas calorimeters that are currently part of CDF [8]. On each "end" of CDF, the plug and forward calorimeters will be replaced with one new end-plug calorimeter. This more compact design will allow us to move the forward muon system closer to the interaction region, thereby increasing our acceptance for muons (see lower Figure 2). The upgraded CDF end-plug calorimeter uses scintillator tiles with fiber readout to photomultiplier tubes as the energy sampling technique. The plug calorimeter upgrade also includes a new fine-grained shower maximum detector to improve electron identification and π^0/γ separation. Table 2 summarizes the features of the new EM calorimeter, Hadron calorimeter and Shower Max Detector.

Table 2
Plug Calorimeter Specifications

EM	Absorber	4.5 mm Pb clad with 0.5 mm stainless steel on both sides
	Scintillator	4 mm Polystyrene
	Total layers	23
	Total thickness	35.7 cm ($23.2\ X_0$, $0.96\ \lambda_{int}$)
	Energy Sampling Fraction	10.4%
	Density	$0.65\ X_0$/cm
	Number of tiles	20448
	Number of towers	960
HAD	Absorber	5.04 cm Fe
	Scintillator	6 mm Polystyrene
	Total layers	22
	Total thickness	160 cm ($6.8\ \lambda_{int}$)
	Energy sampling fraction	2.03%
	Number of tiles	16320
	Number of towers	864
SMD	Scintillator	6 mm Polyvinyltoluene (PVT)
	Total layers	2
	Number of strips	6400

Figure 3 shows a schematic diagram of a scintillating tile read out with a wavelength shifting fiber. Green WLS fibers are glued to scintillating tiles. The green fiber is spliced to a clear fiber which goes out to an optical connector. The optical cables are connected to decoder boxes where light from several tile layers is regrouped so that signals that go to photomultiplier tubes have a tower rather than layer geometry.

The calorimeters are assembled from ϕ sections called "megatiles". The hadron calorimeter megatiles are constructed as follows: First 30° sections are cut from scintillator sheet. A computer-controlled milling machine is used to cut tile separation grooves. The grooves are then filled with a mixture of white paint and epoxy for structural support and to provide a reflective surface at the tile boundaries. Next grooves for the WLS fibers are cut on the tiles. Grooves for WLS fibers and clear fibers are cut on sheets of white plastic matched to the megatile. The plastic layers are placed over the megatiles and the fibers inserted. Finally the megatiles are wrapped in black light tight material and stored in aluminum pans for mechanical protection.

The EM calorimeter megatiles are constructed in a similar manner except that the ϕ sections are 15° and the tiles are individually cut and attached to protective plastic panels using scintillator pins. The

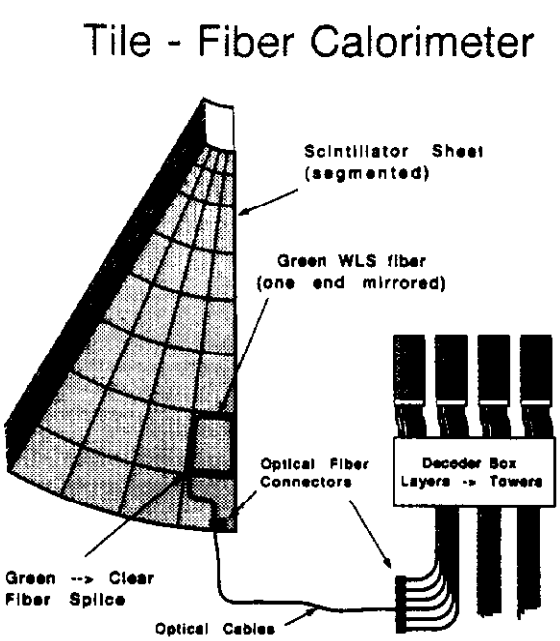

Figure 3. Schematic diagram of a tile-fiber calorimeter.

shower max detector, located six radiation lengths inside the EM calorimeter is constructed of scintillator strips and read out with multi-anode photomultiplier tubes.

An engineering prototype of the new calorimeter was constructed in 1992. It was operated in a test beam and worked well. The construction of the new calorimeter megatiles is now complete and assembly of the EM calorimeter will begin in 1995. The hadron calorimeter will be assembled later since it reuses steel that is part of the existing plug calorimeters. Figure 4 shows the relative light yield from about 12,000 tested tiles.

3. SILICON VERTEX DETECTOR

In 1992, a silicon vertex detector (SVX) was added to CDF. The SVX detected secondary vertices from heavy flavor weak decays - an excellent tool for b tags in top searches and for b-physics. The original SVX was implemented in a "radiation-soft" technology and suffered some degradation due to radiation damage during collider Run Ia. In 1993, we replaced the SVX with a new device, SVX', of similar geometry but using AC-coupled silicon detectors and a radiation-hard readout chip. This detector has also proven

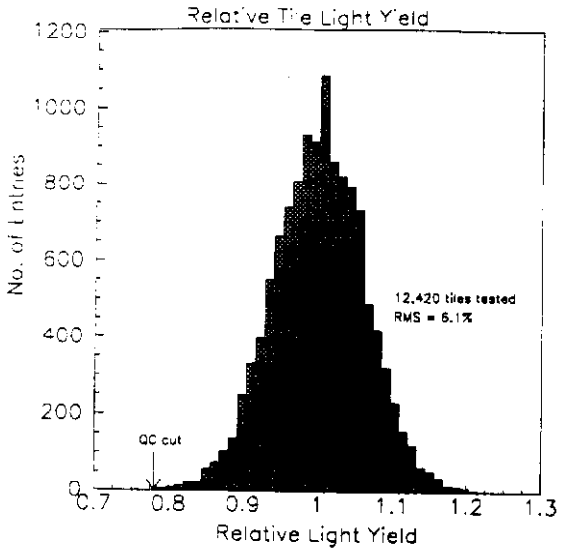

Figure 4. Relative light yield for tiles

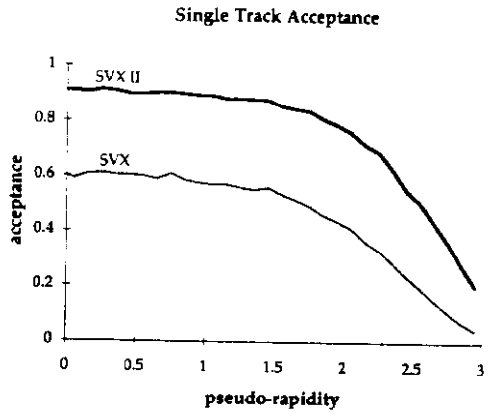

Figure 5. SVX II acceptance vs. pseudo-rapidity.

extremely useful. The SVX' readout chip will not work with the shorter bunch spacing of Run II so the SVX' must be replaced. We call the Run II SVX detector SVX II [9]. The SVX II is designed to address several shortcomings of the SVX':

- The barrel (central) region will be longer to cover the luminous region with higher efficiency (see Figure 5).
- The detectors will be double-sided to provide *r-z* readout for pattern recognition.
- The readout chip will be pipelined for 132 ns bunch spacing.

In addition, information will be available for the trigger. A new Silicon Vertex Tracker will find tracks with large impact parameters to be used in the trigger.

Table 3 compares SVX II design parameters [10] with those of the current SVX. The new detector will consist of three barrels, each 32 cm long. There are 12 wedges in ϕ, each with four layers of silicon. The silicon ladders are mounted between two precision machined beryllium bulkheads. Figure 6 shows a drawing of the detector. The readout chip [11] has 128 channels, each with a charge-sensitive amplifier, pipeline and ADC. We are also exploring the possibility of developing a "deadtimeless" chip which would use a dual-port pipeline scheme so that data acquisition and digitization/readout could occur at the same time.

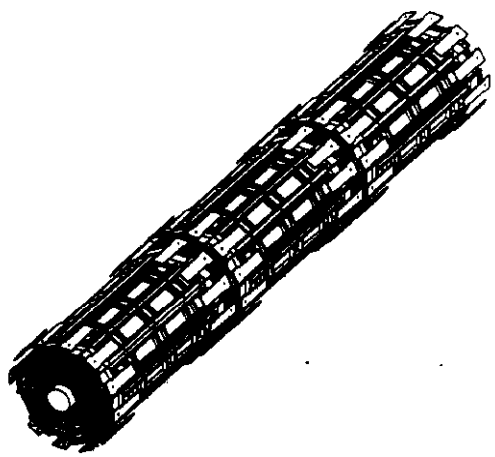

Figure 6. The SVX II detector.

A sketch of the SVX II data acquisition system [12] is shown in Figure 7. Microstrip cables carry the data from the readout chips (on the silicon wafers) to the port cards about 10 cm away. On the port cards, Dense Optical Interface Modules convert the data to optical signals. The data then travels over 10 m low-speed fibers to a Fiber Interface Board. The FIB serializes the data and sends it over high-speed optical fibers to the VME-based data acquisition system.

Table 3
Comparison of SVX and SVX II detector geometries

Detector Parameter	SVX	SVX II
Readout coordinates	r-ϕ	r-ϕ; r-z
Number of barrels	2	3
Number of layers per barrel	4	4
Number of wedges per barrel	12	12
Ladder length	25.5 cm	32.0 cm
Combined barrel length	51.0 cm	96.0 cm
Layer geometry	3° tilt	staggered radii
Radius innermost layer	3.0 cm	2.4 cm
Radius outermost layer	7.8 cm	8.7 cm
r-ϕ readout pitch (4 layers)	60;60;60;55 μm	60;62;58;60 μm
r-z readout pitch (4 layers)	-	150;133;133;150 μm
Length of readout channel (r-ϕ)	25.5 cm	16.0 cm
r-ϕ readout chips/ladder (4 layers)	2;3;4;6	4;6;10;12
r-z readout chips/ladder (4 layers)	-	4;6;6;8
r-ϕ readout channels	46,080	147,456
r-z readout channels	-	110,592
Total number of channels	46,080	258,048
Total number of readout chips	360	2016
Total number of detectors	288	576
Total number of ladders	96	144
Silicon area (m^2)	0.68	1.5
Diode length (miles)	~7.3	~17.2

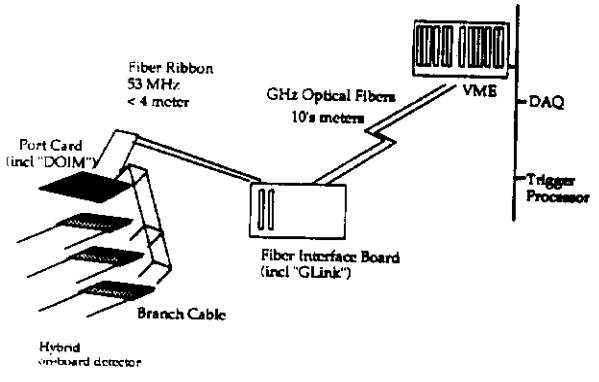

Figure 7. The SVX II Data Acquisition System.

4. ELECTRONICS AND TRIGGER

The front-end electronics for CDF will need to be replaced for Run II to accommodate the reduced bunch spacing. The front-end will have to provide a method of storing events locally, while the lowest level trigger decision is being made. It will be designed to function with bunch spacing as small as 132 ns. The electronics upgrade will include a digital pipeline. Signals from the calorimeter will be digitized every crossing. We plan to use a custom chip to digitize the calorimeter phototube signals [13]. New TDCs will replace the current TDCs used to read out the tracking chambers and muon systems. An advantage of a digital solution is that it becomes very easy to add buffering on the front-end for events passing the lowest level trigger. This will considerably reduce or completely eliminate the dead time associated with the second level trigger. Figure 8 shows the data flow with the upgraded electronics and trigger.

The trigger will be upgraded for Run II to provide a lowest level decision every 132 ns. The decision will be based on threshold requirements for calorimeters and on muon hits. A new track processor is being built since the existing one will not function with the reduced bunch spacing. Buffering will be added at the front end-trigger interface to allow Level 2 operation with little or no dead time. Also, as mentioned above, a new Silicon Vertex Tracker will give us track impact parameter information available at the trigger level.

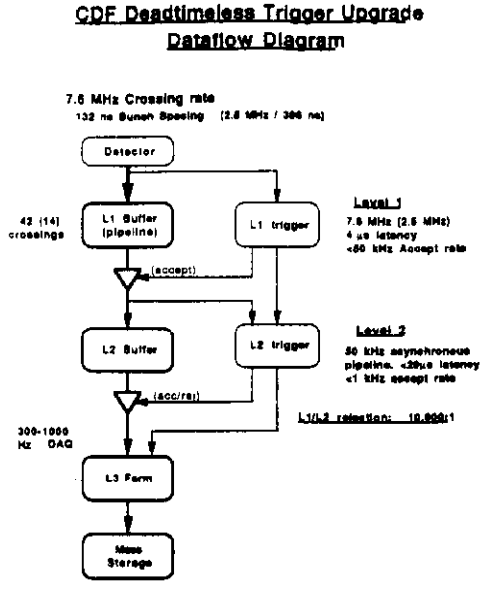

Figure 8. Data flow with upgraded electronics and trigger.

5. DATA ACQUISITION SYSTEM

Finally, we discuss our upgrade of the data acquisition system [14]. This system acquires the digitized data from front-end electronics and delivers it through a high level processor farm (Level 3 system) where the final decision is made to write data to tape and/or on-line monitoring programs. The upgraded system is designed to satisfy the following general requirements:

- Deliver events at the rate of at least 100 Hz to the Level 3 trigger system with a negligible system dead time beyond that due to the Level 2 hardware trigger decision time and due to the front-end digitization time.
- Be partitionable into at least four sections that may be operated in parallel to allow simultaneous debugging of various parts of the detector.
- Be reliable, with down time during data taking periods of less than 5%. Understandable diagnostic information should be provided in case of problems.
- Provide an architecture that can be simply upgraded for higher rates in the future.

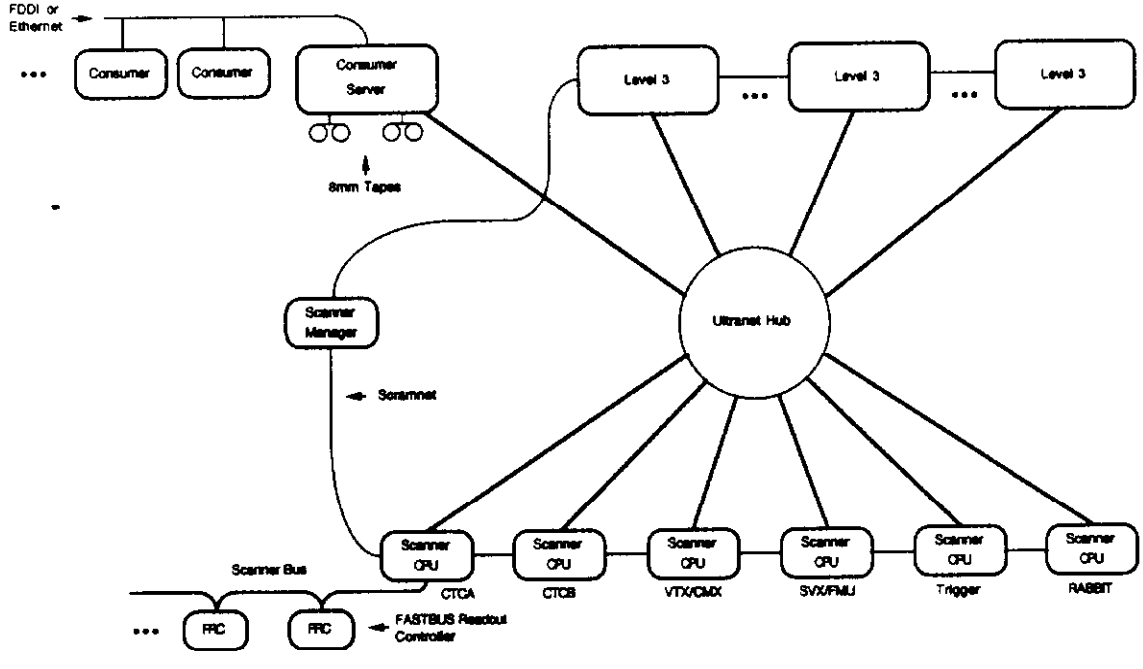

Figure 9. Data Acquisition System Upgrade

A diagram of the new data acquisition system is shown in Figure 9. FASTBUS crates are read out by new FASTBUS Readout Controllers. Other front-end electronics will be read out with VME controllers. Data is collected from the readout controllers with VME-based scanner CPUs. The data are then written through a fast switch to the Level 3 processing farm. Accepted events are routed to a dedicated data logger and consumer server.

A large part of the new data acquisition system has already been installed and is being used for data collection. The new system was needed for the higher rates already present in Run Ib. In addition, the experience gained with the new system now will prove invaluable when the time comes to debug the new front-end electronics.

6. CONCLUSION

Upgrades are essential for CDF to function as the Tevatron luminosity increases and the time between collisions decreases. The CDF upgrade projects will allow us to continue to produce a rich variety of physics results at the high energy frontier.

ACKNOWLEDGMENTS

This work was supported by the U.S. Department of Energy and National Science Foundation; the Italian Istituto Nazionale di Fisica Nucleare; the Ministry of Education, Science and Culture of Japan; the Natural Sciences and Engineering Research Council of Canada; the National Science Council of the Republic of China; and the A.P. Sloan Foundation.

REFERENCES

1. For a recent review of physics results from the Fermilab Collider, see M.J. Shochet, in the Proceedings of the Eighth Meeting of the Division of Particles and Fields of the American Physical Society (DPF '94), University of New Mexico, Albuquerque, NM (1994).
2. S. D. Holmes in Proceedings of the XV International Conference on HIgh Energy Accelerators, World Scientific (1992) 34.
3. See, for example, D. Green and H. Lubatti, (eds.), Physics at Fermilab in the 1990's, World Scientific (1989).
4. F. Abe et al., Phys. Rev. Lett. 73 (1994) 225 and F. Abe et al., Phys Rev. D50 (1994) 2966.
5. Proceedings of the Workshop on B Physics at Hadron Accelerators, (P. McBride and C. Shekhar Mishra, eds., Fermilab-CONF-93/267) contains a wealth of information about both future prospects and existing experimental results for *b* physics at hadron colliders.
6. F. Abe, et al., Nucl. Instrum. and Meth. A271 (1988) 387.
7. D. Amidei et al., Nucl. Instrum. and Meth. A350 (1994) 73.
8. G. Apollinari, P. de Barbaro and M. Mishina in Proceedings of the IV International Conference on Calorimetry in High Energy Physics, La Biadola, Elba, 1993 (FERMILAB-CONF-94/030-E) and S. Aota et al., FERMILAB-PUB-94/244-E.
9. J. Spalding in Proceedings of the 6th Pisa Meeting on Advanced Detectors, Isola d'Elba, Italy (1994).
10. See contributions by J. Skarha and S. Seidel in Proceedings of the Eighth Meeting of the Division of Particles and Fields of the American Physical Society (DPF '94), University of New Mexico, Albuquerque, NM (1994).
11. R. Yarema, FERMILAB-TM-1892.
12. M. Gold in Proceedings of the Eighth Meeting of the Division of Particles and Fields of the American Physical Society (DPF '94), University of New Mexico, Albuquerque, NM (1994).
13. R. Yarema et al., FERMILAB-TM-1895 (1994).
14. J. Patrick in Proceedings of the Conference on Computing in High Energy Physics (CHEP94), S.C. Loken ed., LBL-35822 (1994) 97.